Vibrational relaxation of I_2 in complexing solvents: The role of solvent–solute attractive forces

Joseph J. Shiang, Hongjun Liu, and Roseanne J. Sension[a)]
Department of Chemistry, University of Michigan, Ann Arbor, Michigan 48109-1055

(Received 23 July 1998; accepted 26 August 1998)

Femtosecond transient absorption studies of I_2–arene complexes, with arene=hexamethylbenzene (HMB), mesitylene (MST), or m-xylene (mX), are used to investigate the effect of solvent–solute attractive forces upon the rate of vibrational relaxation in solution. Comparison of measurements on I_2–MST complexes in neat mesitylene and I_2–MST complexes diluted in carbontetrachloride demonstrate that binary solvent–solute attractive forces control the rate of vibrational relaxation in this prototypical model of diatomic vibrational relaxation. The data obtained for different arenes demonstrate that the rate of I_2 relaxation increases with the magnitude of the I_2–arene attractive interaction. I_2–HMB relaxes much faster than I_2 in MST or mX. The results of these experiments are discussed in terms of both isolated binary collision and instantaneous normal mode models for vibrational relaxation. © *1998 American Institute of Physics.* [S0021-9606(98)01245-8]

I. INTRODUCTION

The ability of a fluid to influence chemical reactivity is a function of microscopic transport properties such as viscosity, electrostatic response, and thermal diffusivity. In particular, understanding the ability of a hot solute to transfer energy to a solvent has been the object of numerous experimental and theoretical studies.[1–8] Prior studies have focused on modeling the trends in the vibrational relaxation rate as a function of solvent temperature and pressure.[9,10] Iodine and di-iodide have often been exploited as prototypical systems for such studies of vibrational relaxation.[3,10–15] It is extremely difficult, however, to map theoretical calculations directly onto experimental results, due primarily to the sensitivity of the calculations to the details of the intermolecular potential.[1] The goal of the current study is to examine changes in vibrational relaxation rates as the solute–solvent potential is systematically modified. Specifically, the interaction between iodine and an aromatic solvent is varied by using methyl substitution to tune the degree of I_2–arene charge transfer.

The solution chemistry of I_2 has been studied extensively. I_2 is a model system for photo-induced bond cleavage dynamics and energy relaxation processes in liquids.[2–9,16] Some fraction of the photogenerated I· radicals geminately recombine to form a ''hot'' I_2 species in the ground state. In a noncoordinated solvent the hot I_2 transfers its excess energy to the solvent on 20–40 picosecond time scale.[11,12] Since the optical absorption spectrum of I_2 is extremely well characterized, the progress of this solute–solvent energy transfer can be readily monitored by using time-resolved optical absorption spectroscopy.

The vibrational relaxation of I_2 is also an excellent probe of specific solvent–solute dynamics because the I_2 stretching frequency at $\sim$200 cm^{-1} probes a very specific region of the solvent response spectrum. Low-frequency oscillators such as I_2^- ($\omega \sim 110$ cm^{-1}) probe the peak of the solvent response function for many solvents, and therefore, have rapid population relaxation rates.[13,14] High-frequency oscillators (e.g., C═O) sample multiple solvent events and the combined coupling of inter- and intramolecular motions, and consequently tend to have much slower relaxation rates.[17] The edge of most solvent response functions falls around 200 cm^{-1}, and the relaxation rate of I_2 is accordingly quite solvent sensitive, ranging from a few picoseconds in interacting solvents like mesitylene to $\sim$35 picoseconds in carbon tetrachloride.[11,12]

The interaction between I_2 and arene compounds has an extremely long history providing the prototypical example of a charge-transfer interaction between a donor (the arene) and an acceptor (I_2). In the case of benzene–I_2, the magnitude of charge transfer in the ground state is estimated to be about 0.02 electron charges.[18] The degree of charge transfer can be controlled, however, by substitution on the arene ring. Electron donating methyl groups increase the degree of charge transfer. This increase is manifested both in an increase in $-\Delta H^0$ as more methyl groups are added to the ring,[19] and also as a decrease in the I–I vibrational frequency.[20,21] These trends suggest that methylation of the arene ring provides a sensitive adjustment of solvent–solute interactions.

This paper extends the prior studies of vibrational relaxation of I_2 in mesitylene (MST)[22,23] by examining the vibrational relaxation rate in different solvent environments. Specifically, we present femtosecond transient absorption data on I_2 in m-xylene (mX), I_2 in a 1:5 mixture of MST:CCl_4, and I_2 in mixtures of hexamethylbenzene (HMB):CCl_4, and HMB:cyclohexane. Section II provides a brief overview of the experimental apparatus and conditions. Section III presents an overview of the experimental results. Section IV begins with a review of the formalism developed in a previous paper and concludes with a comparison of the modeled data to two theories of vibrational relaxation. One is the isolated

a)Electronic mail: rsension@umich.edu

binary collision (IBC) theory which regards the solute–solvent interaction as consisting of series of hard-sphere-like collisions.[3,24–27] The other is the instantaneous normal mode (INM) theory which regards the solute–solvent interaction as a single harmonic oscillator (for a diatomic solute) coupled to an ever changing bath of harmonic oscillators.[5–8] These two perspectives emphasize different parts of the potential between molecules, IBC emphasizes the repulsive interactions, while INM emphasizes the attractive interactions. We find that our data is consistent with both models and that the INM model gives an easy and fairly accurate description of the observed experimental trends.

II. EXPERIMENT

The femtosecond laser used to generate the transient absorption data has been described in detail elsewhere.[22] The laser produces pulses which have 350 μJ energy, are 80 fs in duration, and are centered at ~800 nm with a repetition rate of 1 kHz. Half of the output beam is frequency doubled to generate 400 nm excitation pulses. The unconverted fundamental is removed using BG39 Schott glass and the excitation pulse is further attenuated to an intensity of ~800 nJ/pulse. The other half of the laser beam is used to generate a broadband continuum, either in a 1 cm flow cell of ethylene glycol or in a 3 mm sapphire plate. The instrument time resolution was 200 fs (sapphire continuum) or 500 fs (ethylene glycol). For the kinetic data, a 10 nm bandpass interference filter was used to select a portion of the continuum. Spectral data was acquired by passing the continuum through the sample and directing it into a fiber-optically coupled spectrometer while chopping the 400 nm pump beam.[23]

A Raman spectrum was obtained for the HMB:I_2 complex using 30 mW of 532 nm continuous wave excitation from a doubled diode-pumped Nd:YAG laser. The scattered radiation was collected into a 200 mm optical fiber; the other end of the fiber coupled into a SPEX 500M spectrometer equipped with a 2400 groove/mm grating and a Princeton Instruments LN_2 cooled CCD camera. The pixel-to-pixel resolution was 0.75 cm^{-1} and peak positions of I_2 vibrations could be reliably determined to within 1 cm^{-1}. Exposure times of a only a few minutes were necessary. The I_2 frequency for I_2–HMB in CCl_4 is 200 ± 1 cm^{-1}.

All experiments, Raman and time resolved, were collected on liquid samples circulated through a 1 mm quartz flow cell. Freshly prepared samples were exchanged every two hours to prevent a buildup of photoproducts due to sample degradation. The samples were prepared by dissolving solid I_2 (Aldrich, 99.9%) into either the neat arene (m-xylene, MST) or the arene dissolved in cyclohexane or carbon tetrachloride (HMB, MST). The solutions had I_2 concentrations of ~0.01 M.

III. RESULTS

Transient absorption kinetics for I_2 in m-Xylene (mX) and I_2–HMB complexes in CCl_4 and cyclohexane were measured at ten probe wavelengths between 400 and 633 nm. Typical transient absorption kinetics for I_2–HMB in CCl_4 are shown in Fig. 1. The kinetic data obtained for I_2 in m-xylene are qualitatively similar. Data for the I_2–MST complex were reported previously.[22,23] In addition to the kinetic measurements, transient difference spectra were obtained for time delays of 7.5, 10, 15, 25, 50, and 100 ps following excitation of I_2–HMB in CCl_4 and 20, 50, 90, and 200 ps following excitation of I_2 in mX. The difference spectra obtained 7.5 and 100 ps following excitation of I_2–HMB in CCl_4 are shown in Fig. 2. The difference spectra were used to scale the relative magnitudes of the kinetic traces at different wavelengths and to characterize the absorption spectra of the I·–arene complexes.

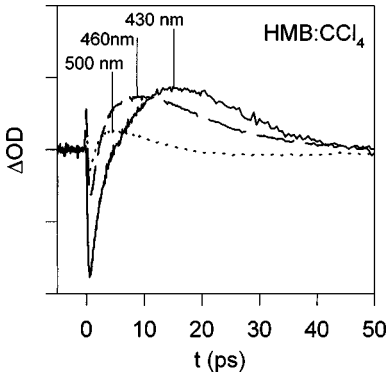

FIG. 1. Transient kinetic measurement obtained at the indicated probe wavelengths following the excitation of I_2–HMB complexes in CCl_4. The pump wavelength was 400 nm.

Prior work on I_2–arene complexes has assigned the different dynamical components present in the transient absorption signal following optical excitation.[22,23,28] There are three major contributions to the data. Two relaxation channels produce highly excited I_2 molecules on the ground electronic state. The electronically excited I_2–arene complexes may undergo rapid dissociation and recombination or internal conversion to the ground electronic state, producing highly excited I_2 on a time scale of 1 to 2 ps. In addition, rapid dissociation of arene–I_2 into arene–I·+I·–arene (or arene–I·+I· in dilute solution) is followed by a partial slow (~15 ps) recombination producing vibrationally excited I_2. The transient difference spectra shown in Fig. 2 are dominated by the visible absorption of I·–HMB complexes. Re-

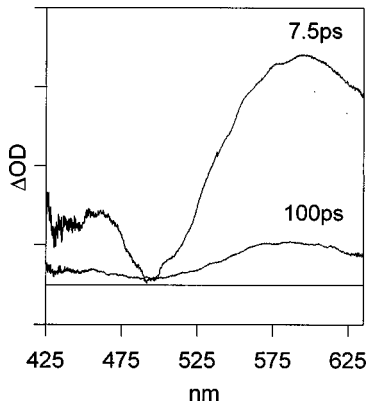

FIG. 2. Transient absorption spectra of I_2 in Hexamethylbenzene:CCl_4 at 7.5 and 100 ps after excitation by a 400 nm pulse. The horizontal line lies at $\Delta OD = 0$.

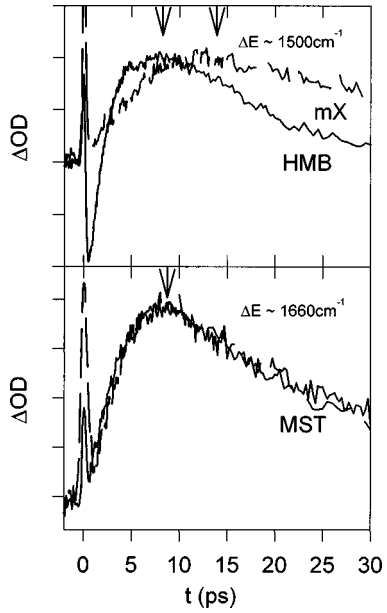

FIG. 3. Transient absorption kinetics following excitation at 400 nm for I_2 complexed to m-xylene, and hexamethylbenzene (top panel) and I_2 complexed to mesitylene both in neat mesitylene and mesitylene diluted in CCl_4 (lower panel). The traces were selected to have approximately the same amount of calculated excess energy (indicated in the top corner of each panel) and correspond to probe wavelengths of 400 nm (m-xylene), 470 nm (hexamethylbenzene), and 430 nm (mesitylene).

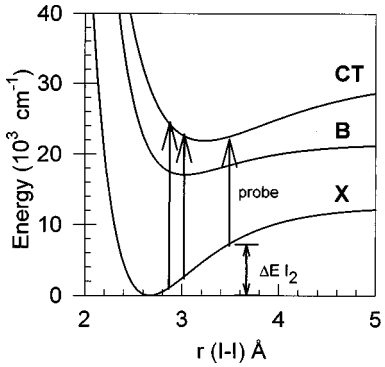

FIG. 4. Morse potential curves for the I–I coordinate with the CT transition as modeled for I_2–MST. The arrows correspond to vertical transitions for ground-state vibrational levels $n=5$, 10, and 40.

combination of I–I in either of these channels results in a signal due to the vibrational relaxation of I_2 in the ground electronic state. In addition to the two relaxation channels producing highly excited I_2, some of the incident photons result in perturbation of the arene–I_2 equilibrium without production of highly excited I_2 molecules.

For I_2–HMB, and the other I_2–arene complexes examined here, the transient absorption from the arene–I· photoproduct is relatively weak in the region of 400–470 nm.[22,23,29] The transient absorption dynamics observed in this region of the spectrum are dominated by vibrational relaxation of I_2–arene complexes.

Transient kinetic data obtained for the three I_2–arene complexes are compared in Fig. 3. The top panel in this figure displays transient absorption traces for I_2 in m-xylene (labeled mX) obtained with a 400 nm probe, and I_2–HMB in CCl_4 (labeled HMB) obtained with a 470 nm probe. The lower panel of Fig. 3 compares the transient absorption signal at 430 nm for I_2 in neat MST with data obtained for a 1:5 dilution of MST in CCl_4. The two kinetic traces almost completely overlap. We have also collected data on the dilute system at 470 nm, and 500 nm and have found a similar close correspondence. Dilution of the MST even further, to 1:15 in CCl_4, also resulted in a kinetic trace at 470 nm that is nearly identical to those collected at higher concentrations. The signals at these wavelengths are dominated by ground-state vibrational relaxation.[23] The similarity between the data obtained at various dilutions leads to the following conclusion: *The local* I_2–arene *interaction dominates the rate at which* I_2 *transfers energy into the solvent.*

Following the procedure developed for I_2–MST in Ref. 3, the delay time to peak absorption may be used to characterize the vibrational relaxation without requiring any additional data manipulation or fitting. Table I shows the delay-to-peak time (in ps) for all of the systems studied here, tabulated between 540 and 400 nm. To convert the experimental probe wavelength into the physically meaningful quantity of excess energy in the I–I bond requires the use of a model for the I_2 potential-energy surfaces. Such a model is shown in Fig. 4. Following the procedure of Ref. 23, we consider three potential surfaces: The ground-state (X), the excited-state (B), and the charge-transfer state (CT) and model them along the I–I coordinate as Morse oscillators. The potential parameters are modified slightly from those used in Ref. 23 to account for shifts in the observed charge-transfer absorption bands. The relevant parameters for HMB and mX are given in Table II and are chosen to best model the static optical absorption spectrum. The use of these potential surfaces permits the assignment of an estimated average excess energy in the I–I bond to each probe wavelength. The result of combining our model for the potential-energy surfaces with the delay-to-peak data in Table I is shown in Fig. 5.

The three kinetic traces compared in Fig. 3 were ob-

TABLE I. Time delay to peak transient absorption as a function of probe wavelength and I_2–arene complex. The time delays are reported in picoseconds.

Wavelength (nm)	540	500	470	460	450	430	400
HMB/CCl_4	3.45	4.9	8.1	9.8	11.5	15	⋯
HMB/c-hexane	2.9	5	6.1	7.2	8	11.5	⋯
MST[a]	2.75	3.75	4.75	⋯	⋯	8.75	12.25
m-xylene	1.6	3.2	4.7	⋯	6.7	7.5	12.8

[a]Data reported in Ref. 23.

TABLE II. Potential parameters for m-Xylene and HMB (given in parentheses where different for m-Xylene). The first four rows refer to Morse potential parameters: $V(r)=D[1-\exp(-\beta(r-r_e))]^2+V_0$. The last row gives the I–arene potential in the CT state according to the equation $V(r)=A/r^{12}-B/r+C$.

State (Bond)	D_e (cm^{-1})	β ($Å^{-1}$)	r_e (Å)	V_0 (cm^{-1})
X(I–I)	12547	1.77(1.73)	2.67	0
X or B (I–Arene)	790(1290)	1.35	3.91(3.78)	⋯
B(I–I)	4382	1.75	3.03	169 18(164 38)
CT(I–I)	8872(7500)	1.16	3.23	208 50(163 80)
	$A(cm^{-1}\,Å^{12})$	$B(cm^{-1}\,Å)$	$C(cm^{-1})$	
CT(I–Arene)	2.596×10^9	8.074×10^4	2.2991×10^4	
	(3.599×10^9)	(1.284×10^5)	(3.702×10^4)	

tained at wavelengths probing similar regions of the ground electronic state potential-energy surface. The probe wavelengths of 400 and 470 nm for I_2–HMB and I_2–mX, respectively, correspond to an approximate excess energy of $\Delta E = 1500\ cm^{-1}$ in the I–I bond. The probe wavelength of 430 nm for I_2-MST corresponds to an approximate excess energy of $\Delta E = 1660\ cm^{-1}$ in the I–I bond. The arrows in this figure indicate the peak of the transient absorption signal at each probe wave length.

Examination of Fig. 5 illustrates that m-xylene–I_2 (open circles) cool at the slowest rates, while the HMB–I_2 complexes (solid symbols) cool the fastest. The identical trend is seen in Fig. 3. For a given value of excess energy, the peak absorption occurs at earlier times for more substituted arenes. The conclusion from both Figs. 3 and 5 is that: *As the degree of methyl substitution is increased, the vibrational cooling rate increases.*

A more quantitative examination of the vibrational relaxation may be made by separating the signal due to vibrational relaxation from the signal attributed to the formation and partial recombination of I·–arene photoproducts. The slow recombination of arene–I· +I·–arene (or arene–I· +I· in dilute solution) to arene–I_2 is prominent in the 550–700 nm region. This recombination may be analyzed by fitting the transient absorption kinetics obtained between 600 and 700 nm. These kinetic traces are well modeled by a single exponential decay of the data to a long-lived plateau resulting from the formation of solvent separated I·–arene radicals. Time constants of 19.5, 14.8, and 11.9 ps are obtained for the recombination channel in mX, MST, and HMB:CCl_4 solutions, respectively. The magnitude of the slow recombination component also varies with solvent. Most of the I–mX complexes undergo cage escape, while the majority of I–HMB undergoes cage recombination. The ratio is ~1:1 in neat mesitylene.[22,23]

The I·–arene difference spectra obtained for time delays of 100 ps or longer may now be used to identify the vibrational relaxation components in the data. The I·–arene photoproduct components are subtracted from the kinetic data obtained at all wavelengths between 425 and 635 nm, by using the parameters obtained from the exponential fits between 600 and 700 nm, scaled according to the relative intensities required by the spectral measurements. The resulting kinetic traces are dominated by the I_2–arene cooling dynamics. Results of this subtraction procedure are shown in Fig. 6. We find in general that the kinetic traces obtained between 400 and 500 nm all have a very large component from vibrational cooling on the ground-state surface.

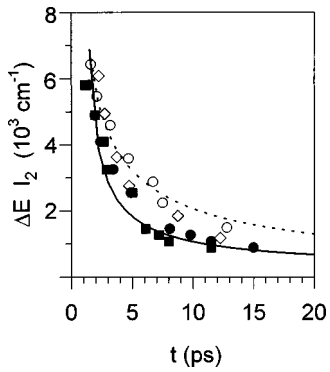

FIG. 5. Average excess energy in the I–I bond plotted as a function of the time delay to peak absorption for the different I_2 complexes examined in this study. Hexamethylbenzene:cyclohexane (solid square), Hexamethylbenzene:CCl_4 (solid circle), mesitylene (open diamond), m-Xylene (open circle). The lines represent the calculated excess energy vs delay based upon the full master equation analysis of the data, solid line: I_2–HMB, dashed line: I_2–mX.

IV. DISCUSSION

A. Master equation modeling of the data

To place our experimental results in the larger context of relaxation processes in liquids in general, it is useful to present a more detailed picture of the cooling process. Following the formalism already developed in the literature,[1,30] and the previous analysis of I_2 relaxation in MST,[23] we will utilize a master-equation approach. The inputs to this approach are the transition rates from each vibrational energy level to all the other levels of the manifold, and some initial nonequilibrium distribution of vibrational energy population. This leads to a set of coupled differential equations

$$\dot{P}_n(t) = -\sum_m k_{n\to m} P_n(t) + \sum_m k_{m\to n} P_m(t), \tag{1}$$

whose initial condition $P_n(0)$, is the initial population distribution. The rate constants are constrained by the requirement of detailed balance

$$\frac{k_{n\to m}}{k_{m\to n}} = e^{-\hbar\omega_{mn}/k_B T}, \tag{2}$$

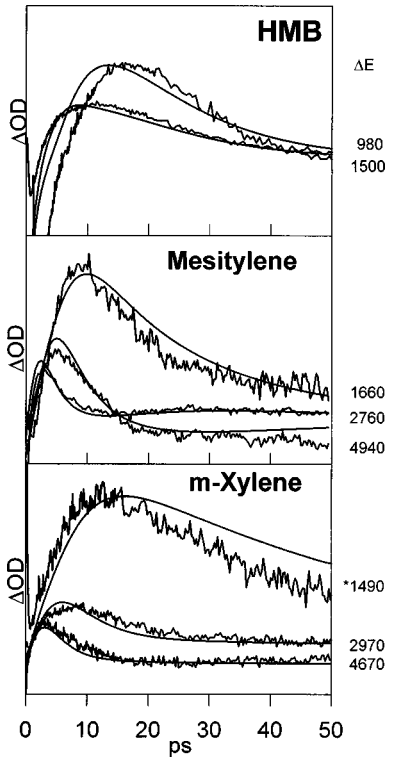

FIG. 6. Kinetic data following removal of the component due to I·–arene recombination. Shown are several kinetic traces for I_2–hexamethylbenzene (top), I_2–mesitylene (middle), I_2–m-xylene (bottom). Indicated by the asterisk is a kinetic trace for which no components were removed (mX, 400 nm probe wavelength). The estimated excess energy in the I_2 bond is given next to each trace. The smooth lines running through the data are the predictions of the master equation model for the population dynamics.

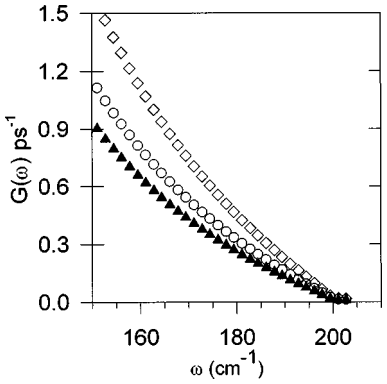

FIG. 7. Experimentally determined power spectrum, $G(\omega)$ for vibrational relaxation of I_2 coordinated to m-Xylene (triangles), mesitylene (circles), and hexamethylbenzene (squares).

$\hbar\omega_{mn}=\hbar(\omega_m-\omega_n)$ is the energy difference between the vibrational level n and m. We write the individual kinetic rate constants for a solute molecule coupled to a bath of oscillators as

$$k_{n\to m}=|\langle n|Q_{nm}|m\rangle|^2 G(\omega_{nm})\left[\frac{1}{e^{\hbar\omega_{nm}/k_BT}-1}+1\right]. \quad (3)$$

The first term on the right side is the dipole transition matrix element between levels of the I–I oscillator. Q_{nm} is the reduced coordinate given by

$$Q_{nm}=\left(\frac{\mu\omega_{nm}}{\hbar}\right)^{1/2} r. \quad (4)$$

For a Harmonic oscillator

$$|\langle n|Q|m\rangle|^2=\frac{n}{2}, \quad m=n-1,$$

$$|\langle n|Q|m\rangle|^2=\frac{m}{2}, \quad m=n+1, \quad (5)$$

$$|\langle n|Q|m\rangle|^2=0, \quad m=\text{otherwise}.$$

The lowest 20 levels of the I–I potential are sufficiently harmonic to consider only transitions between adjacent energy levels. $G(\omega)$ is the spectral response of the solvent which is a convolution of the coupling efficiency of each mode and the solvent density of states. The final term is the Boson occupation number for the modes of the solvent at a frequency ω. $G(\omega)$ thus contains everything needed to model the vibrational relaxation of an oscillator in solution. Our discussion up to this point has been in terms of solvent normal modes, but one may derive an expression for $G(\omega)$ within the context of a collision based master equation model. The resulting expression for $G(\omega)$ differs numerically from its harmonic solvent based cousin only by the phonon occupation factor in Eq. (3).[23,30]

In the previous analysis of MST, $G(\omega)$ was found by optimizing the observed cooling transient at each probe wavelength. Once $G(\omega)$ is known, and an initial population distribution assumed, the population master equation is solved to yield the vibrational population distribution at any given time. The average excess energy in the I–I bond is then

$$\langle\Delta E\rangle=\frac{\Sigma_n P_n(t)E_n}{\Sigma_n P_n(t)}. \quad (6)$$

Given a $G(\omega)$ it is thus possible to calculate the average excess bond energy vs time and compare it to the experimental delay to peak measurement. In order to model the data in Fig. 5, we still need to posit some relationship between the $G(\omega)$ derived for MST [henceforth $G(\omega)^{\mathrm{MST}}$] and the $G(\omega)$ appropriate for other arenes. We shall assume that relationship is that of a simple scaling factor; i.e., the shape of the $G(\omega)$ does not change, only its magnitude does. It turns out that this assumption is all that is needed to model the delay to peak data. Scaling $G(\omega)^{\mathrm{MST}}$ by a factor of 0.81 reproduces the delay to peak data for m-xylene and scaling by a factor of 1.4 fits the delay to peak for HMB dissolved in CCl_4. The three curves for $G(\omega)$ are shown in Fig. 7.

In addition to modeling the delay to peak data, the scaled $G(\omega)$ may also by used to calculate the spectral changes correlated with the cooling dynamics at each wavelength.[23] The predictions of the model are compared to the kinetic data in Fig. 6. Over a wide range of excess energies there is general agreement between model results for both the shape and the relative intensity of the observed cooling components. The one exception is the 1490 cm^{-1} (400 nm probe) m-xylene data, indicated by an asterisk, for which it was necessary to rescale the model intensity. Proper scaling of

TABLE III. Comparison of thermodynamic data, I_2 vibrational frequencies, and the solvent response function for I_2–HMB, I_2–MST, and I_2–mX. The first three rows of the Table summarize spectroscopic and thermodynamic data for the different I_2–arene complexes. The fourth row contains the estimated I–arene force constant (normalized to I–mesitylene) based on thermodynamic and Raman data. The final two rows contain the ratio of $G(\omega)$ for a given I_2 complex (again normalized to mesitylene) for both the experiment and based upon a binary interaction model.

	HMB: c-hexane	HMB: CCl_4	MST: CCl_4	MST	mX	CCl_4
CT λ_{max} (nm)	375	375	335	335	320	⋯
$-\Delta H^0$ (kcal/mol)[a]	4.60	4.60	3.67	3.67	3.12	⋯
$\omega_{gas}-\omega_{solvent}$[b] ($cm^{-1}$)	13.3	13.3	10.8	13.3	11.2	2.0
k/k_{MST}	1.24	1.24	1.0	1.0	0.84	0.19
$G(\omega)/G(\omega)^{MST}$ expt.	1.4	1.4	1.0	1.0	0.81	0.18
$G(\omega)/G(\omega)^{MST}$ INM	1.3	1.3	1.0	1.0	0.77	

[a]Data from Ref. 19.
[b]Data from the present work (HMB) and from Refs. 20 and 21.

this trace is complicated by the fact that it falls outside of the spectral range covered by our transient difference spectra and contains both cooling and recombination components.

B. Relationship to thermodynamic and Raman data

The $G(\omega)$ scaling factors are compared to thermodynamic and Raman data for I_2–arene complexes in Table III. Both of these data sets provide an estimate of the force constant along the I–arene coordinate. If we take the dissociation energy (D) to be equal to $-\Delta H^0$, and use the following Morse oscillator equation for the effective harmonic frequency:

$$\omega=\sqrt{2Dhc\beta^2\mu^{-1}}, \tag{7}$$

then the force constant for this oscillator is $k=\omega^2\mu=2Dhc\beta^2$. *Ab initio* calculations indicate that β does not depend strongly on the degree of methyl substitution on the arene and thus k is roughly proportional to ΔH^0.

The Raman data provide an additional estimate of the changes in the I_2–arene interaction. As the degree of substitution increases the I–I stretching frequency decreases from its gas-phase value of 213.3 cm^{-1}. The magnitude of the observed frequency shift is dependent upon the concentration of the donor–acceptor complex in solution as well as the specific donor involved. The origin of this effect is the weakening of the I_2 bond as electron density is donated into the σ^* anti-bonding orbital. Thus, in neat MST the I–I stretching frequency is 200 cm^{-1}, but when the complex is diluted in CCl_4, the frequency shifts until a final dilute value of 202.5 cm^{-1} is observed.[13] Rosen *et al.* assigned the value of 202.5 cm^{-1} as due to a 1:1 complex, and suggested that lower values of the frequency reflected interactions with an increasing number of MST molecules.[13] Since the weakening of the I–I bond is proportional to the strength of the interaction between the I_2 and the electron donor, the I_2–arene force constant should be proportional to $\delta\omega=\omega_{gas}-\omega_{solvent}$, provided we take into account the effects of multiple interactions with the solvent. Taking the ratio of either ΔH^0 or $\delta\omega$ to their respective values in MST (either neat or diluted in CCl_4, as appropriate) yields a consistent estimate for the relative change in force constant as the degree of substitution is varied. The average of the $\Delta H^0/\Delta H^0_{MST}$ and $\delta\omega/\delta\omega_{MST}$ is listed in the fourth row of Table III as k/k_{MST}.

It is also instructive to scale $G(\omega)^{MST}$ in order to fit the data obtained by Harris *et al.* for the relaxation of I_2 in carbontetrachloride.[11] While there is no reason to believe that the resulting solvent response curve is an appropriate model for CCl_4, this procedure should provide an estimate of the relative strength of the interaction between the arene-complexed iodine and the iodine in an inert solvent. A scaling factor of 0.18 is roughly correct, although the resulting curve is somewhat more biexponential in nature than the data. The trends in Table III clearly indicate a close correlation between the I_2–arene force constant and the observed vibrational relaxation rate.

C. Comparison to models of vibrational relaxation

Our results on both neat and dilute MST suggest that it is the force between a single solvent molecule and the solute which is important and that there is a monotonic relationship between the strength of the solute–solvent force and the rate of vibrational relaxation. To obtain a more quantitative understanding of our results, we compare our results to some of the existing models of vibrational relaxation. We begin by relating the microscopic friction experienced by a solvated, harmonic diatomic, $\eta(\omega)$, to $G(\omega)$[31]

$$\eta(\omega)=\frac{\mu\hbar\omega}{4k_BT}\coth\left(\frac{\hbar\omega}{2k_BT}\right)G(\omega), \tag{8}$$

where μ is the reduced mass of the solute diatomic. At a given temperature, $\eta(\omega)$ is proportional to the previously defined $G(\omega)$. $\eta(\omega)$ is given by Landau–Teller theory as[1(b),8]

$$\eta(\omega)=\frac{1}{kT}\int \cos(\omega t)\langle\delta F\,\delta F(t)\rangle=\left(\frac{\pi}{2}\right)\omega^{-2}\rho(\omega). \tag{9}$$

The middle equation is the classical result of the second fluctuation dissipation theorem.[6,32] To continue, we require some

technique for computing the force autocorrelation function. We first consider an isolated normal mode (INM) picture, and define $\rho(\omega)$ as the ''influence spectrum,'' which is a convolution of the solvent ''density of states'' (which fluctuates in time) and the coupling of each instantaneous mode to the solute vibration; i.e.

$$\rho(\omega)=\sum_{\alpha} c_{\alpha}^{2}\delta(\omega-\omega_{\alpha}), \tag{10}$$

where c_{α} is the coupling constant of each mode to the solute. Focusing attention upon a single solvent normal mode and a single solute bond, c_{α} for an infinitely massive diatomic solute in an atomic solvent is approximately[6]

$$c_{\alpha}^{2}=\sum_{j} \frac{(\mathbf{e}_{\alpha}^{j}\cdot\mathbf{c}_{j})^{2}}{m_{j}}, \tag{11}$$

where the summation is over all j atoms of the solvent, m_j is the mass of each solvent atom, and $\mathbf{e}_{\alpha}^{j}$ is the displacement vector of the jth atom in a normal mode a of the solvent. The vector $\mathbf{c}_j$ is given by

$$\mathbf{c}_{j}=\nabla_{j}\sum_{i=1,2} \frac{(-1)^{i-1}}{2}\,\mathbf{r}_{12}\cdot\nabla u(r_{ij}), \tag{12}$$

where i labels the atoms in the solute bond, $\mathbf{r}_{ij}$ is the bond direction, and $u(r_{ij})$ is the potential between the solvent atom, j, and one of the atoms of the solute, i. For harmonic solvent–solute forces, $\mathbf{c}_j$ is analogous to the force constant. A consequence of Eq. (12) is that the vibrational cooling, at any given time, is dominated by only a few solvent atoms, usually only one or two, which are in the direct vicinity of the solute. While the normal modes are collective motions of several atoms, only the atoms which also have large values of c_{α}^{2} actually make a significant contribution to the relaxation.

The Raman and thermodynamic data (Table III, rows 2 and 3) provide an estimate of the relative change in the magnitude of the force constant between the I_2 and the arene as the degree of methyl substitution is varied. The changes in the force constant, relative to their values in MST, are tabulated in row 4 of Table III. Examination of Eqs. (8)–(12) shows that $G(\omega)$ is proportional to c_{α}^{2}. Based on Ref. 6, we expect the ratio, $G(\omega)/G(\omega)^{\mathrm{MST}}$, to scale as the square of the force constant, given in row 4, divided by the reduced mass of the solvent–I_2 pair. The resulting ratios are given in the sixth row of Table III.

Within the context of the INM model we can rationalize the fact that the cooling rate is independent of dilution while the Raman shift depends upon concentration of charge-transfer complexes. While each surrounding arene linearly contributes to the increase in electron density in the I_2 bond, the influence spectrum scales as the square of the force constants, and thus only the most strongly coupled arene molecule significantly affects the observed relaxation rate. It is also quite striking that the experimentally determined $G(\omega)$ has a steeper slope than that given by a Mori model.[18] This observation is also consistent within the linearly coupled INM model, for one expects the coupling to the solvent to drop dramatically at the point where the one-phonon solvent density of states drops to zero.

It is also possible to reach many of the same conclusions through an isolated binary collision (IBC) perspective. Within the context of the IBC model, the energy loss of a given oscillator is given by[24–27]

$$\Delta E=P\nu, \tag{13}$$

where ν is the ''effective collision rate'' in the condensed phase and P is the amount of energy that each collision removes. The effective collision rate is estimated by:[26]

$$\nu=4\pi\sigma^{2}\rho g(\sigma)\left(\frac{k_{B}T}{\pi m}\right)^{1/2}, \tag{14}$$

Where ρ is the number density, g is the radial distribution function, and σ is the effective cross section. To obtain realistic rates, σ is usually set to a large value, to a region where $g(r)\sim 1$.[26] The large values required suggest that the first solvent-shell number density is the critical parameter and thus it is unlikely that small structural changes would account for the changes in relaxation rates. Furthermore, in order to maintain agreement between the IBC model and our dilution studies, it is necessary to assume that the I_2 is remains closely associated with only one arene during the cooling process, and it this particular arene which is the collision partner for the I_2. If this were not the case, then as the complex is diluted into a more inert solvent such as CCl_4, the collision rate should drop, and the cooling rate should slow appreciably.

The other quantity, P, is usually calculated by summation over classical trajectories of solvent and solute molecules. The summation averages over the solvent thermal velocities as well as the oscillator phase. The interaction between the solvent molecules and the oscillator is usually given by the repulsive wall of the solute–solvent potential. Attractive forces are not explicitly included in the calculation, but, nonetheless, contribute significantly to the relaxation rate. For example, consider the following four parameter potential:

$$V(x)=Ae^{-\alpha x}-Be^{-\beta x}, \quad A,B,\alpha,\beta>0. \tag{15}$$

The purely repulsive part is given by the first term and the second term is purely attractive. For our arena–I_2 we expect that A, α, and β, to remain relatively constant upon methylation but the magnitude of the attractive force, i.e., B, to increase. Performing a Weeks–Chandler–Anderson (WCA) decomposition on the potential[33] and retaining only the repulsive part leads to[27]

$$V(x)=Ae^{-\alpha x}-Be^{-\beta x}, \quad x<\left(\frac{1}{\beta-\alpha}\right)\ln\left(\frac{B\beta}{A\alpha}\right),$$

$$V(x)=0, \quad x\geqslant\left(\frac{1}{\beta-\alpha}\right)\ln\left(\frac{B\beta}{A\alpha}\right). \tag{16}$$

We now fit the resulting WCA potential to the form $V(x)=C\,\exp(-\gamma x)$ and one finds, as one expects, that γ increases

linearly as B is increased. This is significant in light of the Landau–Teller model of vibrational relaxation of a harmonic oscillator which states that[3]

$$P \propto e^{-2\pi\omega/\gamma v_0}, \tag{17}$$

where ω is the oscillator frequency and v_0 is the relative collision velocity. Thus the relaxation rate increase exponentially as γ increases. While this model holds only for the lowest states of the anharmonic I_2 oscillator, it suffices to show that implicit within the operation of an IBC calculation is the inclusion of an attractive force, which scales the magnitude of the solute–solvent repulsive force. A similar conclusion may be reached using a Lennard-Jones potential.[26] The rapid increase in energy transfer with decreasing γ partially explains our MST:CCl_4 dilution experiments, for although collisions between CCl_4 and I_2 must take place, they are much less effective at removing vibrational energy than I_2–MST collisions.

V. CONCLUSIONS

In summary, we have conducted a series of experiments in which the attractive force between solvent and solute is varied. We find that attractive forces modulate the vibrational energy transfer efficiency from solute to solvent. These trends may be understood in terms of either the collision or the normal mode picture. Our data also emphasize the local nature of relaxation processes in solution, which for our model system is dominated by the interaction of the solute with a *single* solvent molecule. In addition, the observed trends in the data support the use of an INM description of solvent–solute interactions.

It would also be worthwhile to extend our current data to encompass a larger range of specific solvent–solute interactions, in order to determine if the force constant scaling we observe holds over a larger range of interaction strengths. In addition, it would be of interest to extend our normal mode analysis to the study of cooling rates in large systems, such as the polyene systems also studied in our laboratory.

ACKNOWLEDGMENTS

This work is supported by a grant from the NSF (CHE-9415772). J.J.S. is supported by the Fellows program of the Center for Ultrafast Optical Science, NSF PHY-8920108.

[1] For recent reviews see: (a) C. B. Harris, D. E. Smith, and D. J. Russell, Chem. Rev. **90**, 481 (1990); (b) J. J. Owrutsky, D. Raftery, and R. M. Hochstrasser, Annu. Rev. Phys. Chem. **54**, 519 (1994).
[2] R. Biswas, S. Bhattacharyya, and B. Bagchi, J. Chem. Phys. **108**, 4963 (1998).
[3] D. J. Nesbitt and J. T. Hynes, J. Chem. Phys. **76**, 6002 (1982).
[4] J. S. Baskin, M. Chachisvilis, M. Gupta, and A. H. Zewail, J. Phys. Chem. A **102**, 4158 (1998).
[5] G. Goodyear and R. M. Stratt, J. Chem. Phys. **105**, 10050 (1996).
[6] R. E. Larsen, E. F. David, G. Goodyear, and R. M. Stratt, J. Chem. Phys. **107**, 524 (1997).
[7] G. Goodyear and R. M. Stratt, J. Chem. Phys. **107**, 3098 (1997).
[8] B. M. Ladanyi and R. M. Stratt, J. Phys. Chem. **102**, 1068 (1998).
[9] D. Schwarzer, J. Troe, M. Votsmeier, and M. Zerezke, J. Chem. Phys. **105**, 3121 (1996).
[10] M. E. Paige and C. B. Harris, J. Chem. Phys. **93**, 3712 (1990).
[11] A. L. Harris, M. Berg, and C. B. Harris, J. Chem. Phys. **84**, 788 (1986).
[12] X. Xu, S.-C. Yu, R. Lingle, H. Zhu, and J. B. Hopkins, J. Chem. Phys. **95**, 2445 (1991).
[13] U. Banin, R. Kosloff, and S. Ruhman, Chem. Phys. **183**, 289 (1994).
[14] P. K. Walhout, J. C. Alfano, K. A. M. Thakur, and P. F. Barbara, J. Phys. Chem. **99**, 7568 (1995).
[15] R. Zadoyan, Z. Li, P. Ashjian, C. Martens, and V. Apkarian, Chem. Phys. Lett. **218**, 504 (1994); J. Chem. Phys. **101**, 6648 (1994).
[16] J. Franck and E. Rabinowitch, Trans. Faraday Soc. **30**, 120 (1934); E. Rabinowitch and W. C. Wood, *ibid.* **32**, 547 (1936).
[17] P. Moore, A. Tokmakoff, T. Keyes, and M. D. Fayer, J. Chem. Phys. **103**, 3325 (1995).
[18] J. Lascombe and M. Besnard, Mol. Phys. **58**, 573 (1986).
[19] B. B. Bhowmik and S. P. Chattopadhyay, Spectrochim. Acta A **37**, 135 (1981).
[20] W. Keifer and H. J. Bernstein, J. Raman Spectrosc. **1**, 417 (1973).
[21] H. Rosen, Y. R. Shen, and F. Stenman, Mol. Phys. **22**, 33 (1971).
[22] S. Pullen, L. A. Walker II, and R. J. Sension, J. Chem. Phys. **103**, 7877 (1995).
[23] H. J. Liu., S. H. Pullen, L. A. Walker II, and R. J. Sension, J. Chem. Phys. **108**, 4992 (1998).
[24] D. W. Oxtoby, Mol. Phys. **34**, 987 (1977).
[25] J. Chesnoy and J. J. Weis, J. Chem. Phys. **84**, 5378 (1986).
[26] P. S. Dardi and R. I. Cukier, J. Chem. Phys. **89**, 4145 (1988); **86**, 6893 (1987); **86**, 2264 (1987).
[27] D. J. Russell and C. B. Harris, Chem. Phys. **183**, 325 (1994).
[28] E. Lenderink, K. Duppen, F. P. X. Everdij, J. Mavri, R. Torre, and D. A. Wiersma, J. Phys. Chem. **100**, 7822 (1996), E. Lenderink, K. Duppen, and D. A. Wiersma, Chem. Phys. Lett. **211**, 503 (1993).
[29] E. F. Hilinski and P. M. Rentzepis, J. Am. Chem. Soc. **107**, 5907 (1985).
[30] N. Pugliano, A. Z. Szarka, S. Gnanakaran, M. Triechel, and R. M. Hochstrasser, J. Chem. Phys. **103**, 6498 (1995).
[31] Equation (11) of Ref. 1(b) gives an expression for $k_{n,n-1}$ in terms of $\eta(\omega)$ which we then combine with Eqs. (3) and (5).
[32] I. Benjamin and R. M. Whitnell, Chem. Phys. Lett. **204**, 45 (1993).
[33] D. Chandler, J. D. Weeks, and H. C. Anderson, Science **220**, 787 (1983).